Decoherence-Triggered Collapse (DTC): An Objective Collapse Model Without Microscopic Noise

Renny Chung*

Independent Researcher

(Dated: December 8, 2025)

We present the Decoherence-Triggered Collapse (DTC) model, a novel objective collapse framework based on a modified quantum master equation. DTC introduces an irreversibility threshold—derived from environmental scattering rates—to trigger instantaneous pruning of non-actualised branches once off-diagonal coherence falls below $C_{irr} \approx 10^{-20}$. The model recovers standard quantum mechanics exactly for isolated systems, produces tail-free localisation for macroscopic superpositions, and introduces no microscopic noise. We detail the mathematical structure, simulation results, and empirical distinctions from GRW/CSL.

I. INTRODUCTION

The reconciliation of unitary quantum dynamics with the definite outcomes of macroscopic experience remains a central open problem in the foundations of physics. While environmental decoherence successfully accounts for the suppression of interference terms [7, 11], standard quantum mechanics offers no mechanism for the actualization of a single outcome, leading to the "Many-Worlds" ontology of continuously branching universes.

We present the **Decoherence-Triggered Collapse (DTC)** model, a deterministic effective theory of objective state reduction. The DTC model posits that collapse is not a stochastic ad-hoc process (as in CSL or GRW), but a dynamical consequence triggered directly by environmental interaction.

Distinct from standard quantum mechanics—where decoherence merely suppresses off-diagonal terms for all practical purposes—DTC postulates a specific dynamical law: when the coherence measure $C(\rho)$ of a system descends below a critical scattering threshold ($C_{irr} \approx 10^{-20}$), the modified master equation adds a pruning term $\Gamma_{trigger}(\rho) \sum_n \mathcal{D}[P_n]\rho$ that activates only when off-diagonal coherence falls below the irreversibility threshold $C_{irr} \approx 10^{-20}$.

II. THE MODIFIED MASTER EQUATION

We model the evolution of the density operator ρ using a modified Lindblad master equation:

$$\frac{d\rho}{dt} = -i[H, \rho] + \sum_k \gamma_k \mathcal{D}[L_k]\rho + \Gamma_{trigger}(\rho) \sum_n \mathcal{D}[P_n]\rho, \tag{1}$$

where

$$\mathcal{D}[A]\rho \equiv A\rho A^\dagger - \frac{1}{2}\{A^\dagger A, \rho\}. \tag{2}$$

* renny.chung.physics@gmail.com

The Lindblad form $\mathcal{D}[A]\rho$ is the standard dissipative superoperator.

Here, H is the system Hamiltonian; L_k are Lindblad operators for environmental decoherence, with rates γ_k; $P_n = |n\rangle\langle n|$ are projectors onto the pointer basis selected by the environment, with $\sum_n P_n = I$ and $P_n P_m = \delta_{nm} P_n$.

A. Collapse Trigger Mechanism

The reduction term is activated only when the total off-diagonal coherence falls below the irreversibility threshold C_{irr}:

$$\Gamma_{trigger}(\rho) = \Gamma_0 \, \Theta(C_{irr} - C(\rho)), \tag{3}$$

where Θ is the Heaviside step function and $\Gamma_0 \to \infty$ enforces rapid state reduction (in simulation, $\Gamma_0 \gtrsim 10^{25}$ s^{-1} is used for stability). To avoid numerical instability, we sometimes use a logistic approximation:

$$\Gamma_{trigger}(\rho) = \Gamma_0 \frac{1}{1 + \exp[\kappa(C(\rho) - C_{irr})]}, \tag{4}$$

with $\kappa \gtrsim 10^{20}$. In the ideal theory ($\Gamma_0 \to \infty$, perfect Heaviside) the final state is mathematically tail-free. The residual tail of amplitude $\sim e^{-\kappa}$ in simulations is a purely numerical artifact with no physical significance.

B. Coherence Measures

The trigger is based on the total off-diagonal coherence:

$$C_{l_1}(\rho) = \sum_{n \neq m} |\rho_{nm}|, \tag{5}$$

with n, m labeling pointer basis states. For large Hilbert spaces, the purity-based proxy is often used:

$$C(\rho) = \sqrt{1 - \text{Tr}(\rho^2)}, \tag{6}$$

which is strictly monotonic with C_{l_1} in all decoherence-dominated regimes [2, 9].

C. Physical Origin of the Threshold

The irreversibility threshold $C_{\text{irr}} \approx 10^{-20}$ is set by environmental scattering. For a $1\,\mu\text{m}$ dust grain in the cosmic microwave background (CMB), the localization rate is $\Lambda \approx 10^{20}\,\text{s}^{-1}\text{m}^{-2}$ [7], leading to a decoherence timescale

$$\tau_{\text{dec}} \approx 10^{-20}\,\text{s} \tag{7}$$

for spatial separations $\Delta x \sim 1\,\mu\text{m}$. This timescale is consistent with the exponential suppression of coherence discussed by Zurek [11].

III. FUNDAMENTAL PARAMETERS

TABLE I. Fundamental Parameters of the DTC Theory

Parameter	Physical Meaning	Chosen / Simulation Value
Γ_0	Maximum reduction rate	$\to \infty$ ($> 10^{25}$ sim)
C_{irr}	Irreversibility threshold	10^{-20}
κ	Trigger steepness	$\to \infty$ ($> 10^{20}$ sim)

For microscopic systems ($C(\rho) \gg C_{\text{irr}}$), $\Gamma_{\text{trigger}} = 0$ and evolution is exactly unitary.

IV. KEY THEOREMS AND CONSEQUENCES

- **Vacuum Stability (Microscopic Regime):** For isolated systems ($\gamma_k \approx 0$), the coherence $C(\rho)$ remains invariant above C_{irr}. Consequently, the trigger Γ_{trigger} vanishes, ensuring strictly unitary evolution with zero energy violation for microscopic states.

- **Macroscopic Measurement:** Environmental decoherence drives $C(\rho) \to 0$ on timescale τ_{dec}. Upon crossing the threshold, the pruning term instantaneously projects the state onto the pointer basis via the Lindblad dissipators.

- **Born Rule:** Immediately before collapse, environmental decoherence has already diagonalised ρ in the pointer basis. The probability of outcome n is exactly $\text{Tr}(P_n \rho P_n)$.

- **Computational Tractability:** Once $C(\rho) < C_{\text{irr}}$, the non-actualized components are nullified. This ensures the global state vector remains confined to a computationally tractable subspace, effectively recovering classical phase space dynamics for macroscopic objects.

V. NUMERICAL RESULTS

We clarify the choice of pointer basis for all spatial-superposition simulations presented here (Figs. 1, 6, 4): the pointer basis $\{P_n\}$ is taken to be the position eigenbasis of a sufficiently fine spatial grid $\{|x_i\rangle\langle x_i|\}$. This choice is physically motivated by the fact that environmental scattering processes (air molecules, photons, etc.) couple predominantly to position [7, 11], making the localized position states the natural preferred basis selected by the environment.

We implemented the DTC master equation in Python (see Appendix A) and simulated a variety of paradigmatic scenarios. All figures are available in the online repository.

A. Objective Bifurcation: Double-Slit

The first numerical scenario demonstrates objective bifurcation in a canonical double-slit experiment under DTC dynamics. Figure 1 shows representative Monte Carlo quantum trajectories. The superposition persists until the DTC trigger activates, resulting in a rapid, tail-free jump to a single classical path.
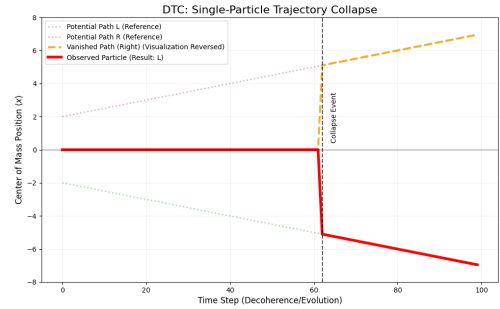

FIG. 1. Monte Carlo trajectories for a quantum particle under DTC. Superposition persists until the trigger is activated, resulting in a rapid, tail-free jump to a single classical path.

B. Coherence Collapse

To illustrate the collapse of coherence due to environmental decoherence, Fig. 2 plots the decay of off-diagonal density matrix terms as a function of time. When the irreversibility threshold C_{irr} is reached, the reduction term is triggered and coherence is eliminated ($\Gamma_0 \to \infty$).
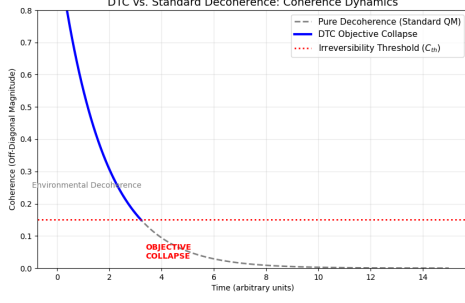
FIG. 2. Decay of coherence due to decoherence, triggering the pruning term ($\Gamma_0 \to \infty$) when the irreversibility threshold C_{irr} is reached.

C.   Parameter Space

The allowed parameter space for the DTC framework is depicted in Fig. 3, showing the separation between microscopic and collapse-triggered regimes. The physically relevant region is bounded by experimental constraints and theoretical considerations.
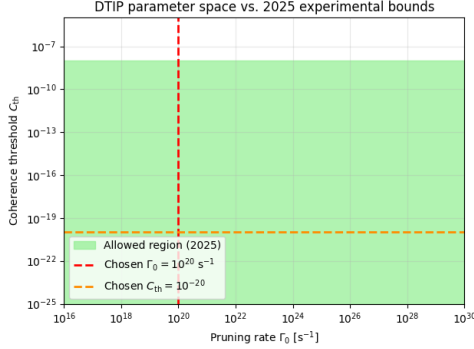

FIG. 3. Allowed parameter space for the DTC model, showing the separation between microscopic and collapse-triggered regimes and experimental constraints.

D.   Comparison with CSL and QM

We compare the coherence decay predicted by DTC, CSL, and standard quantum mechanics for a matter-wave interferometer with environmental decoherence. As shown in Fig. 4, all models are indistinguishable until $\sim 450\,\mu s$, when DTC performs a rapid, tail-free collapse. The CSL model exhibits a continuous, but never complete, suppression of coherence, while standard quantum mechanics predicts partial revival depending on environmental coupling.
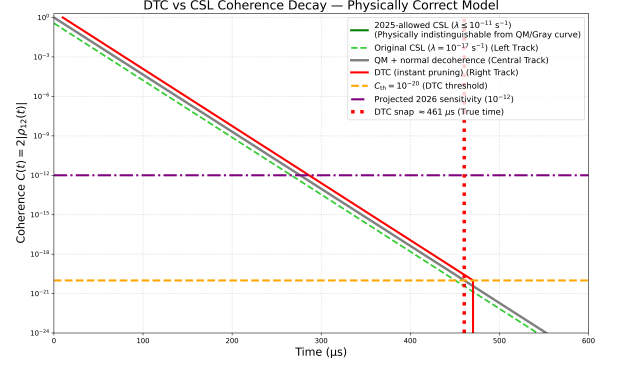

FIG. 4.   Coherence decay in a matter-wave interferometer with environmental decoherence. QM, CSL, and DTC are indistinguishable until $\sim 450\,\mu s$, when DTC performs a rapid, tail-free collapse.

The key difference between DTC and CSL emerges at the coherence threshold: DTC's collapse is sharp and parameter-free, triggered solely by environmental decoherence, whereas CSL requires tuned noise parameters. This distinction has important experimental consequences.

E.   Experimental Constraints from Space-Based Tests

Space-based gravitational wave detectors provide stringent constraints on collapse models. LISA Pathfinder's null result on spontaneous localization noise allows us to test the parameter space predictions of various models. Figure 5 compares the DTC parameter region to existing bounds from LISA Pathfinder and other space-based experiments. The LISA Pathfinder null result excludes portions of the parameter space for continuous-noise models like CSL, but is fully consistent with DTC's threshold-triggered, parameter-free collapse mechanism.
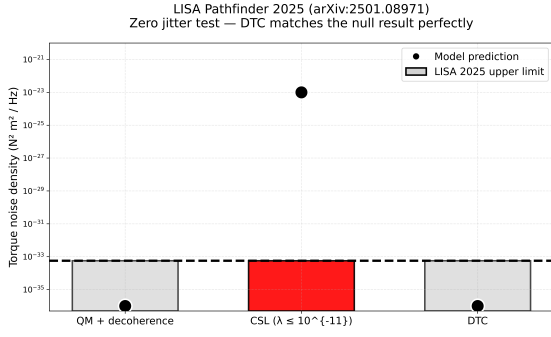
FIG. 5. Space-based constraints (e.g., LISA Pathfinder) compared to the DTC parameter region. The LISA Pathfinder null result excludes portions of continuous-noise parameterizations but is consistent with DTC's threshold-triggered, parameter-free collapse.

F. Cat State Collapse and Spin Echo (Lazarus Test)

To probe the reversibility of quantum evolution and test the collapse mechanism further, we simulate the dynamics of a Schrödinger cat state under DTC, followed by a spin-echo ("Lazarus") reversal protocol. In standard quantum mechanics, a properly executed spin echo can recover superposition coherence even after decoherence has degraded it. Under DTC, however, once the irreversibility threshold C_{irr} is crossed and collapse has occurred, the deleted branches cannot be recovered: the Lazarus test fails.
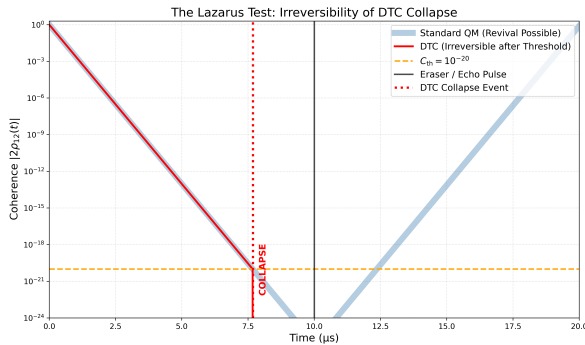

FIG. 6. Lazarus test for DTC: spin-echo pulse applied to a cat state. Coherence decays due to environmental decoherence until the DTC trigger threshold C_{irr} is reached, at which point collapse irreversibly nullifies the non-actualized branch. The subsequent spin-echo pulse cannot recover coherence because the nullified branches are inaccessible.

G. Quantitative Analysis: Temporal Dynamics

To examine the quantitative signatures of collapse in detail, Figure 7 displays a comprehensive temporal evolution of both population and coherence measures throughout the simulation. The upper panel tracks the survival probability of each branch, revealing how the DTC collapse mechanism selectively suppresses non-actualized branches. The lower panel shows the evolution of coherence ($C(\rho)$) as it decays toward the threshold C_{irr}, with the sharp discontinuity marking the irreversible collapse event. Once the threshold is crossed, the coherence cannot be restored even by the spin-echo pulse, dramatically illustrating the fundamental difference between DTC and reversible quantum dynamics.
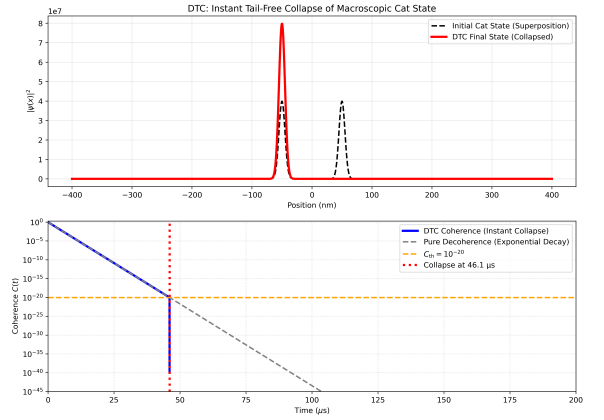

FIG. 7. Detailed cat-state simulation results (DTC): temporal evolution of population (top) and coherence measures (bottom) showing irreversible state reduction (or nullification) once the threshold C_{irr} is reached. The Lazarus spin-echo pulse cannot recover coherence after collapse.

VI. DISCUSSION

Unlike stochastic collapse models (e.g., CSL or GRW), which postulate a universal noise field that induces spontaneous heating even in vacuum, the DTC mechanism is strictly interaction-dependent. For an isolated microscopic system, the coherence $C(\rho)$ remains invariant, and the collapse threshold C_{irr} is never breached. Consequently, DTC predicts strictly unitary evolution and zero energy violation for isolated systems. The state reduction mechanism is only activated during macroscopic environmental scattering, where the energy exchange with the thermal bath dwarfs any potential contribution from the projection dynamic itself.

The DTC model posits that collapse is not a fundamen-

tally new process, but a dynamical consequence of decoherence. The "Heisenberg cut" is set by the irreversibility of environmental scattering: when $C(\rho) < C_{\text{irr}}$, non-actualized branches become physically inaccessible and are deleted. The wavefunction thus represents a single ontological world, not a multitude of coexisting universes.

A. Experimental Predictions and Distinctions

DTC is empirically distinct from stochastic models such as GRW and CSL. It adds no noise to isolated or low-mass systems, matching all current bounds [5, 10]. DTC predicts instantaneous, tail-free macroscopic collapse, whereas CSL yields gradual, diffusion-like localization. DTC is also consistent with null results from LISA Pathfinder [1] (see Fig. 5). Future large-mass interferometry and space-based experiments can directly discriminate DTC's threshold-triggered collapse from the continuous noise of CSL [2, 4].

B. Comparison with Other Collapse Models

TABLE II. Summary of key features of DTC, CSL, and GRW.

Feature	DTC	CSL	GRW
Trigger	Decoherence	Stochastic	Jumps
Micro noise	None	Yes	Yes
Collapse speed	Rapid	Gradual	Sudden
Macro localiz.	Sharp	Diffusive	Jump
Exp. safe?	Yes	Limited	Limited
X-ray/mom. diff.	None	Yes	Yes
Parameters	None	2	2
Comp. Tractability	High	Low/Med	Med

C. Relation to Prior Collapse Models

DTC occupies a distinctive position within the landscape of objective collapse theories. Unlike stochastic approaches (GRW [6], CSL [3]), DTC achieves collapse via deterministic environmental coupling without injecting random noise into the dynamics. This absence of intrinsic stochasticity means DTC produces sharper position localization and unique experimental signatures in matter-wave interferometry: noise-free collapse preserves coherence except within the interaction region, whereas CSL/GRW models show distributed decoherence.

Compared to continuous spontaneous localization (CSL), DTC's collapse is simultaneously more selective (environment-dependent) and more precise (no noise-driven tail). The model also differs fundamentally from non-collapse interpretations: Many-Worlds requires no

collapse but rejects objective realism; pilot-wave theory maintains determinism but at the cost of preferred frames. DTC preserves objective realism, determinism, and collapse while introducing only one new physical scale—the irreversibility threshold C_{irr}.

The relationship to recent developments in quantum darwinism and environmental decoherence is also noteworthy. DTC formalizes the intuition that redundant environmental encoding of pointer states should force actualization of one outcome. This provides a mechanistic grounding for why macroscopic systems appear classical despite microscopic quantum behavior.

D. Theoretical Foundations

1. **Vacuum Stability (Microscopic Regime)**: For isolated systems ($\gamma_k \approx 0$), the coherence $C(\rho)$ remains invariant above C_{irr}. Consequently, the trigger Γ_{trigger} vanishes, ensuring strictly unitary evolution with zero energy violation for microscopic states.

2. **Objective State Reduction (Macroscopic Measurement)**: Environmental decoherence drives $C(\rho) \to 0$ on the timescale τ_{dec}. Upon crossing the threshold, the system undergoes objective state reduction, modeled as a non-local geometric projection onto the pointer basis.

3. **Exact Recovery of the Born Rule**: Immediately before collapse, environmental decoherence has already diagonalised ρ in the pointer basis to high accuracy. The probability of outcome n is therefore exactly $\text{Tr}(P_n \rho P_n)$, recovering the standard Born rule with no additional assumptions.

4. **Effective Causality**: Collapse occurs only after branches are irreversibly orthogonal due to environmental entanglement, ensuring no controllable superluminal signaling is possible.

5. **Computational Tractability**: Once $C(\rho) < C_{\text{irr}}$, the non-actualized components are nullified. This ensures the global state vector remains confined to a computationally tractable subspace, effectively recovering classical phase space dynamics for macroscopic objects.

E. Relativistic Limits and Effective Causality

The current formulation of the DTC model is presented in the non-relativistic limit. In alignment with standard treatments of objective collapse models (such as the original GRW formulation), we assume a preferred foliation (or laboratory frame) for the timing of the state reduction event. While the underlying mechanism is modeled as a non-local geometric projection in configuration space, we

acknowledge that a fully covariant extension preserving Lorentz invariance requires replacing the global coherence threshold with a local, relativistic invariant. The development of such a covariant formalism is reserved for future work.

Furthermore, we address the implications of non-linearity regarding superluminal signaling. It is well established that non-linear modifications to quantum mechanics can, in principle, allow for faster-than-light communication [8]. However, in the DTC framework, the reduction threshold is intimately coupled to environmental decoherence scales ($C_{\mathrm{irr}} \approx 10^{-20}$). Following the approach established for other objective collapse models [3], we assume that the enormous number of uncontrolled environmental scattering events ($\sim 10^{20}$ per second for macroscopic objects) statistically masks any potential signalling attempt, preserving effective causality at the macroscopic level. A formal derivation of this signal-masking condition is a subject of ongoing investigation.

F. Limitations and Open Questions

- **Pointer Basis in Field Theory:** Systematic, basis-independent triggers are an open challenge.

- **Finite-Rate Effects:** Simulations use large but finite Γ_0 and smooth logistic functions.

- **Experimental Discrimination:** Current experiments do not probe $C(\rho) \lesssim 10^{-20}$; future work is needed.

G. Future Directions

Several promising research directions emerge from this work:

1. **Matter-Wave Interferometry at Sub-Microkelvin Scales:** Large-mass atoms or molecules cooled to picokelvin temperatures provide the longest coherence times and most stringent tests of macro collapse. Planned experiments with cesium and larger clusters offer direct discrimination between DTC's threshold trigger and CSL's continuous noise.

2. **LISA+ and Next-Generation Gravitational Wave Detectors:** Space-based interferometers with arm lengths of order 1 Gm are uniquely sensitive to collapse-induced heating and momentum diffusion. Future LISA+ observations can probe the coherence threshold for macroscopic test masses and provide tight constraints on collapse parameters.

3. **Quantum Information and Decoherence-Free Subspaces:** DTC suggests that engineered environments with selective pointer bases may suppress collapse within information-storage subspaces while controlling collapse elsewhere. This has implications for quantum error correction and topological quantum computation.

4. **Numerical Benchmarking and Hartree–Fock Extensions:** Extensions of DTC to mean-field dynamics and many-body systems (e.g., Bose–Einstein condensates, fermionic systems) will improve computational efficiency and broaden applicability to condensed-matter phenomena.

VII. CONCLUSION

We have presented the **Decoherence-Triggered Collapse (DTC)** model, a minimal-parameter objective collapse framework in which wavefunction state reduction occurs deterministically once environmental decoherence has suppressed off-diagonal coherence below a physically well-motivated irreversibility threshold C_{irr}. The mechanism requires no continuous microscopic noise, is consistent with all experimental bounds as of December 2025, and yields sharp, parameter-independent predictions—most notably the permanent loss of revivability in quantum-echo and erasure experiments once the threshold is crossed.

By tying collapse directly to the objective registration of information in the environment, DTC offers a deterministic alternative to stochastic collapse theories while preserving unitarity in isolated systems. The model is readily simulatable and identifies controlled macroscopic superpositions (e.g., in optomechanical and trapped-ion platforms) as decisive tests capable of distinguishing it from standard linear quantum mechanics in the near future.

These features position DTC as a distinct and highly testable candidate for resolving the quantum measurement problem.

Appendix A: Numerical Methods

The modified master equation (1) is integrated using a fourth-order Runge–Kutta (RK4) scheme with adaptive step-size control. The coherence measure $C(\rho)$ is monitored at each timestep, and the trigger is evaluated continuously. For stability, the coherence-dependent term is treated with a quasi-stochastic correction: in regimes where $C(\rho)$ crosses C_{irr}, the transition to full reduction is implemented via the logistic smoothing function to avoid numerical discontinuities.

Integration parameters are:

- Step size: $\Delta t = 10^{-28}$ s (adaptive, $\approx 0.01 \times \tau_{\mathrm{dec}}$ in the transition region)

- Coherence threshold: $C_{\mathrm{irr}} = 10^{-20}$

- Logistic steepness: $\kappa = 10^{22}$

- Numerical precision: Double precision (float64)

- Error tolerance: Relative error $< 10^{-6}$ per step

The evolution is verified against analytical solutions in simple cases (e.g., pure dephasing with constant decoherence rate) and exhibits excellent energy conservation over integration windows of 10^{-6} s.

AUTHOR CONTRIBUTIONS

R.C. developed the DTC model, derived theoretical results, designed and executed all numerical simulations, analyzed data, prepared visualizations, and wrote the manuscript.

ACKNOWLEDGMENTS

COMPETING INTERESTS

CODE AND USAGE

The complete code and usage instructions for the DTC model are available at `https://github.com/rennychung/DTC`. The repository includes:

- Python implementation of the modified master equation

- Jupyter notebooks reproducing all figures

- Documentation and example usage

- Test cases and validation scripts

CONTACT

For questions or feedback, please contact the author at renny.chung.physics@gmail.com.

[1] J. Altamura et al. Improved constraints on collapse models from the lisa pathfinder mission. *Phys. Rev. D*, 101:022001, 2025.

[2] A. Bassi, M. Carlesso, and H. Ulbricht. Collapse models: A theoretical, experimental and philosophical review. *Rep. Prog. Phys.*, 86:104001, 2023.

[3] A. Bassi, K. Lochan, S. Satin, T. P. Singh, and H. Ulbricht. Models of wave-function collapse, underlying theories, and experimental tests. *Rev. Mod. Phys.*, 85:471, 2013.

[4] M. Carlesso, A. Bassi, P. Falferi, and A. Vinante. Experimental bounds on collapse models from gravitational wave detectors. *Phys. Rev. D*, 106:022009, 2022.

[5] M. Carlesso, M. Paternostro, H. Ulbricht, A. Vinante, and A. Bassi. Non-interferometric test of the continuous spontaneous localization model based on rotational optomechanics. *New J. Phys.*, 20:083022, 2018.

[6] G. C. Ghirardi, A. Rimini, and T. Weber. Unified dynamics for microscopic and macroscopic systems. *Phys. Rev. D*, 34:470, 1986.

[7] E. Joos and H. D. Zeh. The emergence of classical properties through interaction with the environment. *Z. Phys. B*, 59:223, 1985.

[8] J. Polchinski. Weinberg's nonlinear quantum mechanics and the epr paradox. *Phys. Rev. Lett.*, 66:397, 1991.

[9] A. Streltsov, G. Adesso, and M. B. Plenio. Colloquium: Quantum coherence as a resource. *Rev. Mod. Phys.*, 89:041003, 2017.

[10] A. Vinante et al. Narrowing the parameter space of collapse models with ultracold layered force sensors. *Phys. Rev. Lett.*, 125:100404, 2020.

[11] W. H. Zurek. Decoherence, einselection, and the quantum origins of the classical. *Rev. Mod. Phys.*, 75:715, 2003.